water

MDPI

Article

Mapping Groundwater Potential Zones Using Analytical Hierarchical Process and Multicriteria Evaluation in the Central Eastern Desert, Egypt

Mohd Yawar Ali Khan [1,*], Mohamed ElKashouty [1,*] and Fuqiang Tian [2]

[1] Department of Hydrogeology, Faculty of Earth Sciences, King Abdulaziz University, Jeddah 21589, Saudi Arabia
[2] Department of Hydraulic Engineering, School of Civil Engineering, Tsinghua University, Beijing 100084, China; tianfq@tsinghua.edu.cn
* Correspondence: makhan7@kau.edu.sa (M.Y.A.K.); melkashouty@kau.edu.sa (M.E.)

Abstract: Exploring alternative freshwater resources other than those surrounding the Nile is critical to disperse Egypt's population to other uninhabited desert areas. This study aims to locate groundwater potential zones (GWPZs) in the water-scarce desert between the Qina and Safga-Bir Queh regions to build groundwater wells, thereby attracting and supporting people's demand for water, food, and urban development. Multi-criteria evaluation (MCE) and analytical hierarchical process (AHP) techniques based on remote sensing (RS) and Geographic Information System (GIS) were used to map GWPZs. The outcome of the GWPZs map was divided into six different classes. High and very-high aquifer recharge potentials were localized in the middle and western parts, spanning 19.3% and 17% (16.4% and 15.7%) by MCE (AHP). Low and very low aquifer recharge potentials were distributed randomly in the eastern part over an area of 29% and 14.3% (26.9% and 6.1%) by MCE (AHP). Validation has been undertaken between the collected Total Dissolved Solid (TDS) and with the calculated GWPZs, indicating that the highest and lowest TDS concentrations of most aquifers are correlated with low to very low and high to very high aquifer potential, respectively. The study is promising and can be applied anywhere with similar setups for groundwater prospect and management.

Keywords: GWPZs; RS&GIS; multi-criteria evaluation; analytical hierarchical process; TDS; Egypt

Citation: Khan, M.Y.A.; ElKashouty, M.; Tian, F. Mapping Groundwater Potential Zones Using Analytical Hierarchical Process and Multicriteria Evaluation in the Central Eastern Desert, Egypt. *Water* **2022**, *14*, 1041. https://doi.org/10.3390/w14071041

Academic Editors: Ataur Rahman and Abdullah Al Mamun

Received: 23 February 2022
Accepted: 23 March 2022
Published: 25 March 2022

1. Introduction

Egypt has a rapidly growing population of around 100 million people who live on less than 6% of the country's land area [1]. As a result, the demand for water, food, and urban development is rapidly increasing. These circumstances necessitate the development of new, favorable locations in Egypt that have not yet been developed. The Eastern Desert accounts for 20% of Egypt's total land area. The Nile Valley is bounded east by the Gulf of Suez and west by the Red Sea. The Safaga-Bir Queh region is located in the Eastern Desert's central region. It holds an important position because it overlooks the Red Sea, providing access to the Gulf States, East Asia, and Africa. It is a vast, dry area with scarce groundwater resources. It is an attractive new investment area in the Egyptian deserts for irrigation practice. Climate change refers to any statistically significant and persistent change in the mean state of the climate over a long period. Social migration influences the local immigrants. Climate variability can relate to changes in natural or anthropogenic external factors and natural internal processes within the climate system. The world has just passed through the frightening state of increasing temperature at a pace of 0.128 ± 0.026 °C each year for 59 years, with its negative impact on global vegetation cover [2]. In unplanned economic activities, precipitation affects soil moisture. Moisture content differs from soil to soil and season to season, influenced by rainfall. Surface water

resource management and an area's physiographic characteristics are necessary for humans and agricultural use. Ecosystem activities and agricultural planning have been deemed a vital sector in irrigation planning by policymakers worldwide due to their importance in agriculture. Climate change's hydrological response may considerably influence existing water resources systems by altering the hydrological cycle. As a result, hydrologic extremes such as flooding and drought have a harmful influence on all watersheds. However, planning and organizing the new water infrastructure are not developed according to the projected changes of precipitation, temperature, and stream flows for efficient water resource management.

New agricultural projects in the desert have attracted densely populated residents of the River Nile area (Qena). From 1960 to 1996, the per capita annual water availability in the Arab countries declined to 2050 m^3 [3]. Due to the sharp increase in population, it is evident that other water consumed in the next 30 years will altogether diminish. It is crucial to detect and investigate the most promising aquifer recharge areas in response to this situation. People will agree to reside in the desert if there will be a proper arrangement of groundwater resources, infrastructures, and agriculture. The groundwater resources are not enough to irrigate the land between the Qena and Safaga-Bir Queh area; therefore, modern techniques are necessary to explore new groundwater potential zones (GWPZs). Part of the desert land is used for water-consuming crops and partly for medicinal herbs (low water consumption). There is a significant impact of anthropogenic activities on groundwater quality and quantity in urban and rural zones. Therefore, there is a need to provide alternative groundwater resources.

The actual supply of water was insufficient to meet demand. As a result, there is an urgent need to develop alternative water resources, which are the main objective of the present work. Watersheds in the Eastern Desert dissect into the Red Sea Mountains and extend into Cretaceous and Tertiary rocks, eventually draining into the Red Sea or the Nile Valley [4]. The average precipitation ranges from 2.75 mm/y at Qena to 50 mm/y in the extreme southeastern zone, with heavy rain showers occurring on occasion during the autumn season, causing flooding. Despite the scarcity of rainfall events, many flash floods were reported in both the Eastern Desert and Sinai between 1975 and 2014 [3,5]

The aquifers are among the most critical water resources for growth and drinking suitability in rural and urban areas [6]. The aquifer was always migrated and rechargeable, but unfortunately, it is rare in hard rocks (geology of the present study). Modern geophysical, geological, and hydrogeological surveys techniques are currently used to find new and promising groundwater recharge areas, but they are complex, costly, and require consultants [7]. Hydrogeological and geological thematic maps overlap with remote sensing (RS) and Geographic Information System (GIS) techniques have been used for several past investigations [8,9]. GIS and RS techniques are combined to determine the aquifer's recharge zone [10–12]. RS and GIS tools can detect the most promising recharge areas for aquifer [13–16]. The groundwater prospection zones are based mainly on integrations of multiple criteria such as stream networks, topography, lithology, and steepness of slope and frequency of lineaments. This process is most commonly known as multi-criteria evaluation (MCE) [17]. They represent good evidence of aquifer conditions [18]. AHP for delineating GWPZs has been used by researchers in Kedah Peninsula, Malaysia [19]. The authors of [20–23] used the analytical hierarchical process (AHP) techniques for the exploration of GWPZs and recharge rate. The AHP technique declines the complicated outputs to a sequence of pair-wise data and produces the results [24]. The AHP is an excellent approach for calculating outputs consistency, decreasing bias, and applying in a different environment [20]. The features, such as geomorphology, geology, lineaments density, slope, drainage density, and rainfall, are integrated by the GIS model with weightage determination by AHP to produce aquifer potential and recharge zones.

Due to the arid to the very arid climatic nature, the shortage of freshwater is the main problem affecting development plans in the Qena and Safaga-Bir Queh region of the eastern desert in Egypt. Groundwater is a preferred alternative solution to deal with this type of

problem, but >50% of the covered geology was hard rocks; therefore, the aquifer potential delineation and distribution geospatially was very complex due to the shortage in data sets and geological changes. Therefore, this study aims to determine the distribution of shallow aquifers suitable for living, agriculture, and industrial development by evaluating aquifer influencing parameters, discovering aquifer recharge zones, and finally, creating a GWPZs map using and comparing AHP and MCE techniques based on RS and GIS. In addition, the observed total dissolved solid (TDS) in the groundwater of the study area has been used to validate the model outputs of potential aquifer zones. The study shows the significance of the AHP and MCE technique for preparing an efficient and low-cost approach for delineating GWPZs, which may also be applied in other hard rock terranes.

2. Materials and Methods

2.1. Study Area

The Eastern Desert include about one-fourth of Egypt's area and covers an area of 222,117 km^2 approximately and is considered an arid area. The investigated area (triangle in shape) has about 4238 km^2 and lies between latitudes 26°0′0″ N to 27°0′0″ N and longitudes 32°40′0″ E to 34°20′0″ E in the central part of the Eastern Desert (Figure 1).

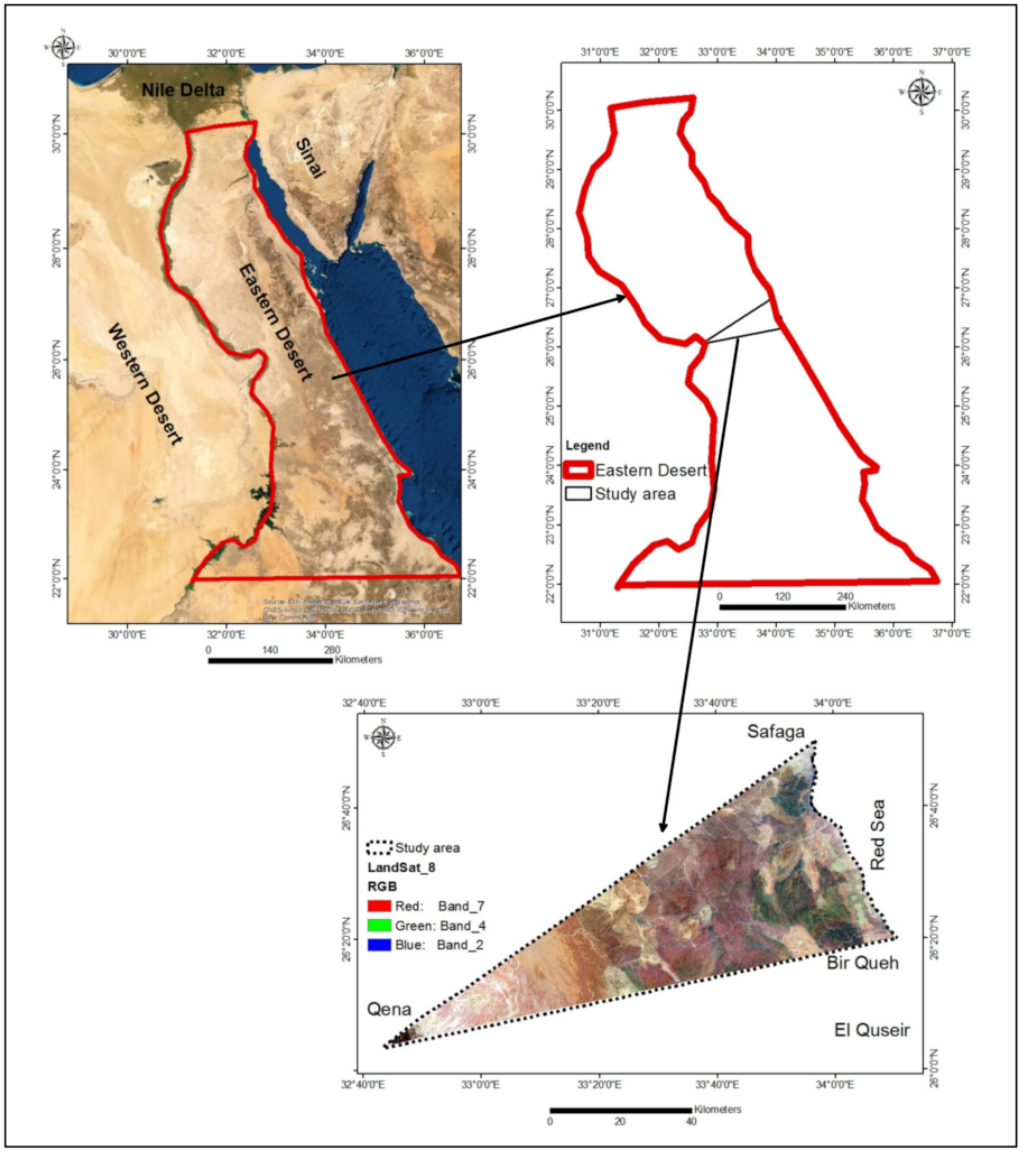

Figure 1. Location map of the study area (Qena-Safaga-Bir Queh), Eastern Desert, Egypt.

The central region of the Eastern Desert has a dry climate with an aridity degree of 0.2284, long hot summers, and short warm winters [25]. The maximum temperature ranges from 23 °C in winter to 42 °C in summer, with a mean annual temperature of 25 °C. The average yearly rainfall in the western part of the central Eastern Desert is around 3.94 mm, while about 4 mm in the eastern region. In November 1994, an unusual rainfall event of 25 mm occurred, resulting in a dangerous flash flood [25]. Throughout the year, the humidity in Safaga ranged between 40% and 60%, while it ranged between 15% and 14% in Qena.

Geology and Hydrogeology

The geology of the study area mainly consists of crystalline and sedimentary rocks (Figure 2). The Precambrian basement complex (crystalline rocks) has the same direction of movement as the Red Sea graben. It is composed mainly of igneous and metamorphic sediments [26–28]. The Lower Cretaceous (Nubian sandstone) consists of sandstone, shale, and clay. The Nubian sandstone is capped by aquitard (Upper Cretaceous shale) and underlain by basements complex.

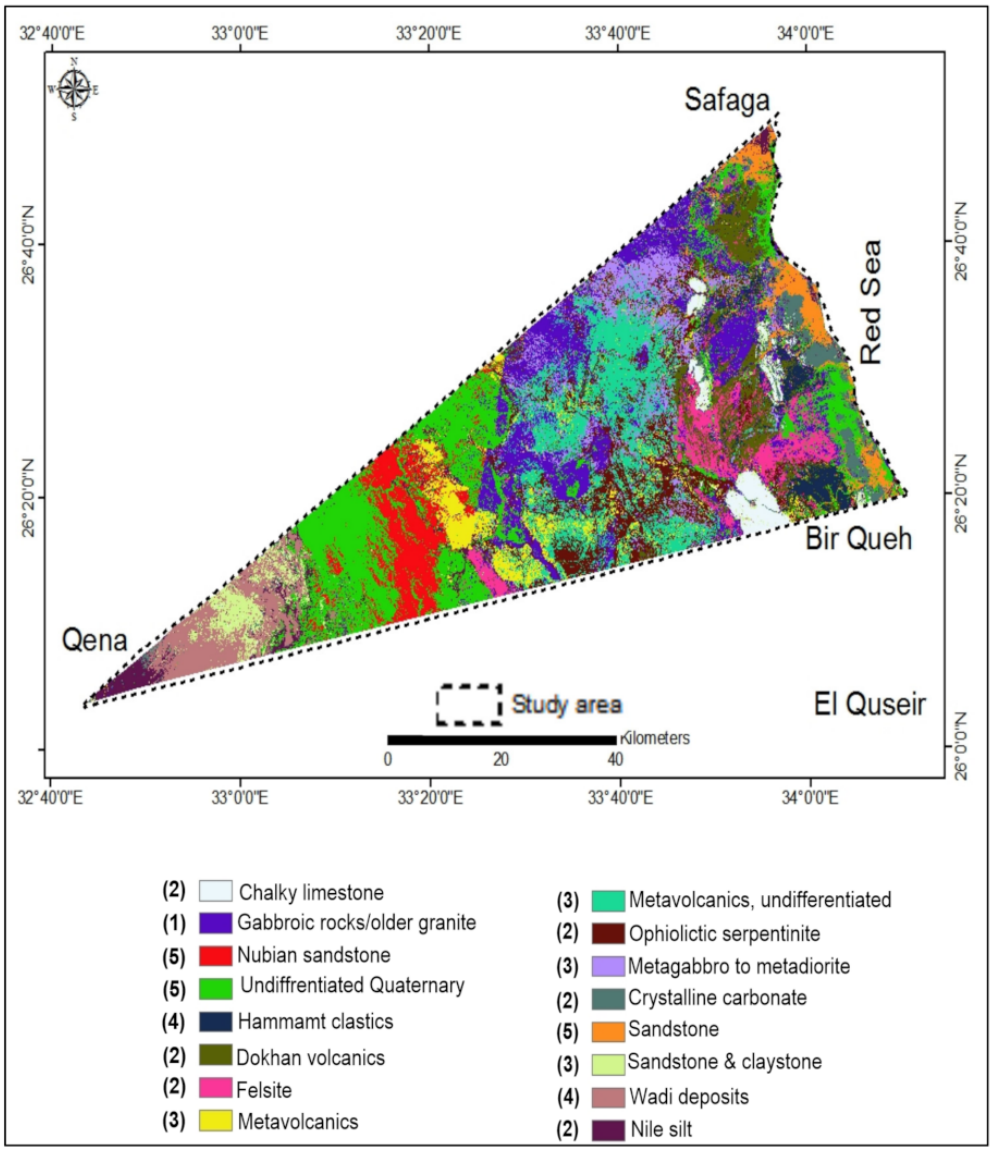

Figure 2. Classified (digitized) geological map of the study area (number 1–5 (very low–very high)) shows the aquifer potentiality. Geology after [29].

The Post-Nubian is differentiated into carbonate, Neogene, and alluvial deposits (Figure 3).

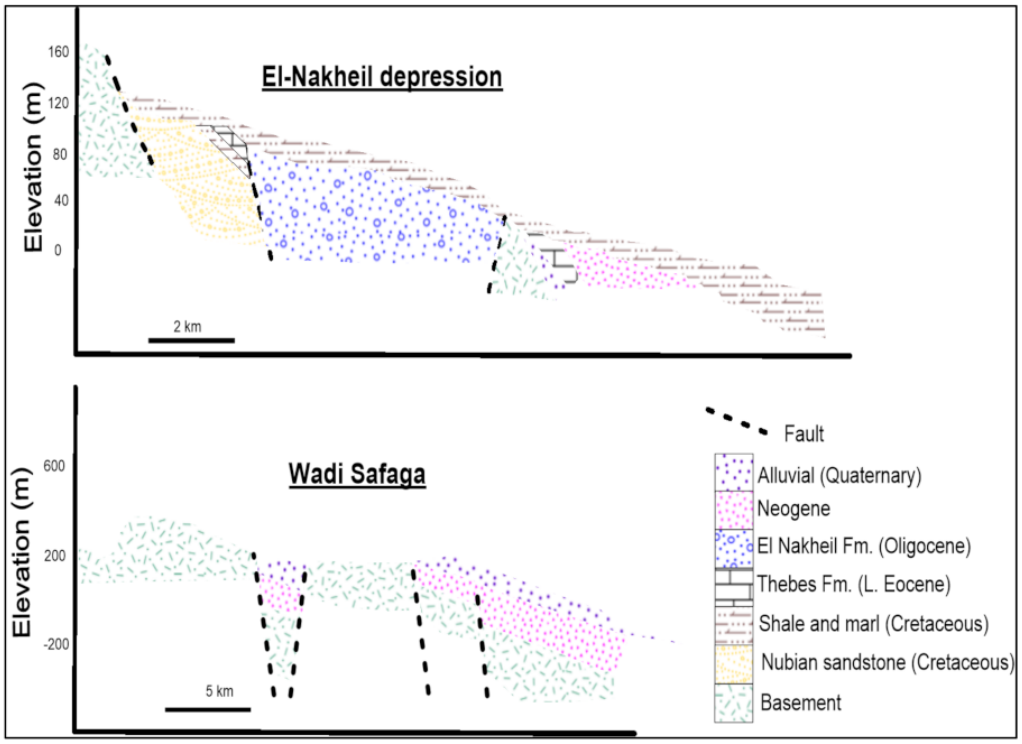

Figure 3. Geological cross-section along El Nakheil and Wadi Safaga [30].

In Figure 2, older granite and gabro rocks covered most of the study area, followed by serpentine ophiolite, Nubian sandstone, and Dukhan volcano, while Cretaceous limestone covered a small portion [31]. Carbonate rocks have partly been characterized by conduits (bedding planes and structural impact), increasing aquifer storage (Figure 2). The Eastern Desert represents one of the four major segments of Egypt (parallel crustal plates) separated by the NNW-SSE fault trends [32]. It is characterized by faults, folds, and volcanic formations. Groundwater occurrences in the study area are rare compared to other parts of Egypt. It is due to the crystalline rock, which covers almost all parts while the precipitation decreases. The clay and shale alternate with sandstone and sands in the Nubian aquifer. The depth of the water and the thickness of the aquifer are 4–40 m and 10–120 m, respectively. In the Middle Miocene (Neogene), the discharge rate, transmissivity, storativity, and permeability of sandstone aquifer are 480 m^3/day, 187.1 m^2/day, 1856 $\times$ 10^{-7}, and 11.69 m/day, respectively [33], with a water depth (WD)of 17 m [34]. In the Oligocene, the discharge rate, transmissivity, storativity, and permeability of aquifer are 432 m^3/day, 133.99 m^2/day, 0.000698, and 2.26 m/day, respectively, at the upstream region, and 432 m^3/day, 1364 m^2/day, and 0.0444 and 10.12 m/day, respectively, at the downstream region. The Quaternary sediments were exposed at the mainstream and their branches, constructing terraces at the coast of the River Nile. The Quaternary aquifer is of poor quality due to its small thickness, unconfined nature, and seawater intrusion. The WD ranges from 5.2–11.8 m [34]. Figure 4 shows the average WD and TDS of the aquifers at the Safaga-El Quseir area [34]. The TDS of groundwater in Wadi Qena ranges from 1191–5507 mg/L and 1496–1715 mg/L in Quaternary and Nubian aquifers, respectively [33].

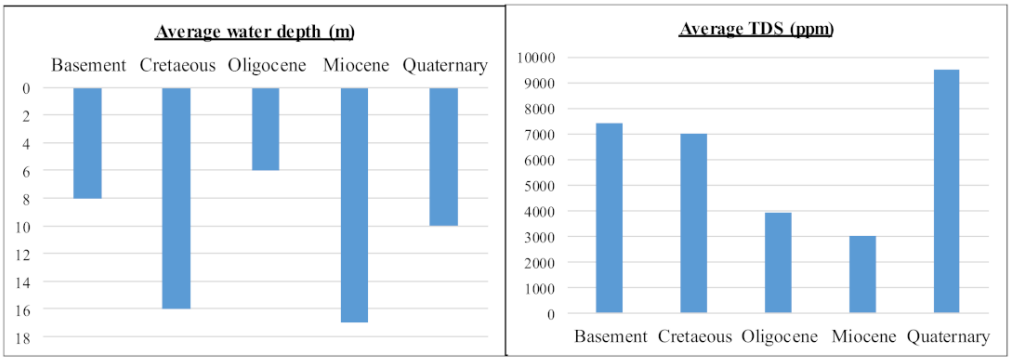

Figure 4. Average water depth and TDS of the aquifers at Safaga-El Quseir area [35].

2.2. Data Sets

Three images of Shuttle Radar Topography Mission–Digital Elevation Model (SRTM-DEM) namely SRTM1N26E032V3 (Coordinates: 26, 32), SRTM1N26E033V3 (Coordinates: 26, 33), and SRTM1N26E034V3 (Coordinates: 26, 34) were downloaded from United States Geological Survey (USGS) website (http://earthexplorer.usgs.gov/; accessed on 20 September 2021). Two ETM+ (Enhanced Thematic Mapper Plus) images of Landsat-8 having path 174/row 42 (LC08_L1TP_174042_20151115_20170402_01_T1) and path 175/row 42 (LC08_L1TP_175042_20151106_20170402_01_T1) with 30 m resolution (suitable for DEM and lineaments analyses) were also downloaded from the USGS websites (http://earthexplorer.usgs.gov/; accessed on 20 September 2021).

2.3. Methodology

The DEM images were mosaicked using ArcGIS 10.3 software to represent the investigated study area. There are 11 bands in the ETM+ images, and there is little cloud cover (0.02). The wavelengths, atmospheric velocity, UTM projection WSG84, and anisotropy of the ETM+ images have all been corrected. Geological maps [36] at a scale of 1: 250,000 were scanned and georeferenced using satellite imagery coordinates. The supervised image classification accuracy assessment Maximum Likelihood (ML) classifier was used to distinguish and digitize the various exposed rock units. ETM+ images were used to create a base map for each region. For digital image processing, ENVI v 5.1 software is used.

The data is preprocessed to create a mosaic of images. Rainfall, lithology, rock fractures (linear lines), slopes, and drainage density were extracted for MCE using ArcGIS 10.3 software tools. Extraction (Envi v 5.1); automatic extraction lineaments (using PCI Line); handling extraction lineaments (Arc GIS 10.3); and trend analysis (RockWork v 16) are the lineament delineation steps. The principal component image (PCI) contains the most information and is best suited for lineament extraction (PCI Geomatica). In ArcGIS 10.3 software, DEM images and other source data were used to create thematic maps (geomorphology, geology, lineaments density, slope, drainage density, and rainfall for MCE). According to classification, attribute values are assigned to each theme.

Using the UTM-WGS 84 (36 N) projection coordinate system, all layers were projected. Thematic maps were reclassified and converted into raster images with a weight scale ranging from 1 to 5 (see Tables S1 and S2). The classes were assigned based on their contribution to aquifer recharge potentiality, ranging from very high to very low. Weighted overlay analysis was used to combine the output raster maps. The overlay analysis (prospect map) was divided into five categories ranging from very low to very high potentiality.

Figure 5 illustrates the methodologies adopted for this study, which are MCE and AHP. GWPZs was correlated with groundwater salinity (TDS) to validate the outputs and determine the accuracy. The TDS concentration of aquifers data was collected from [37,38].

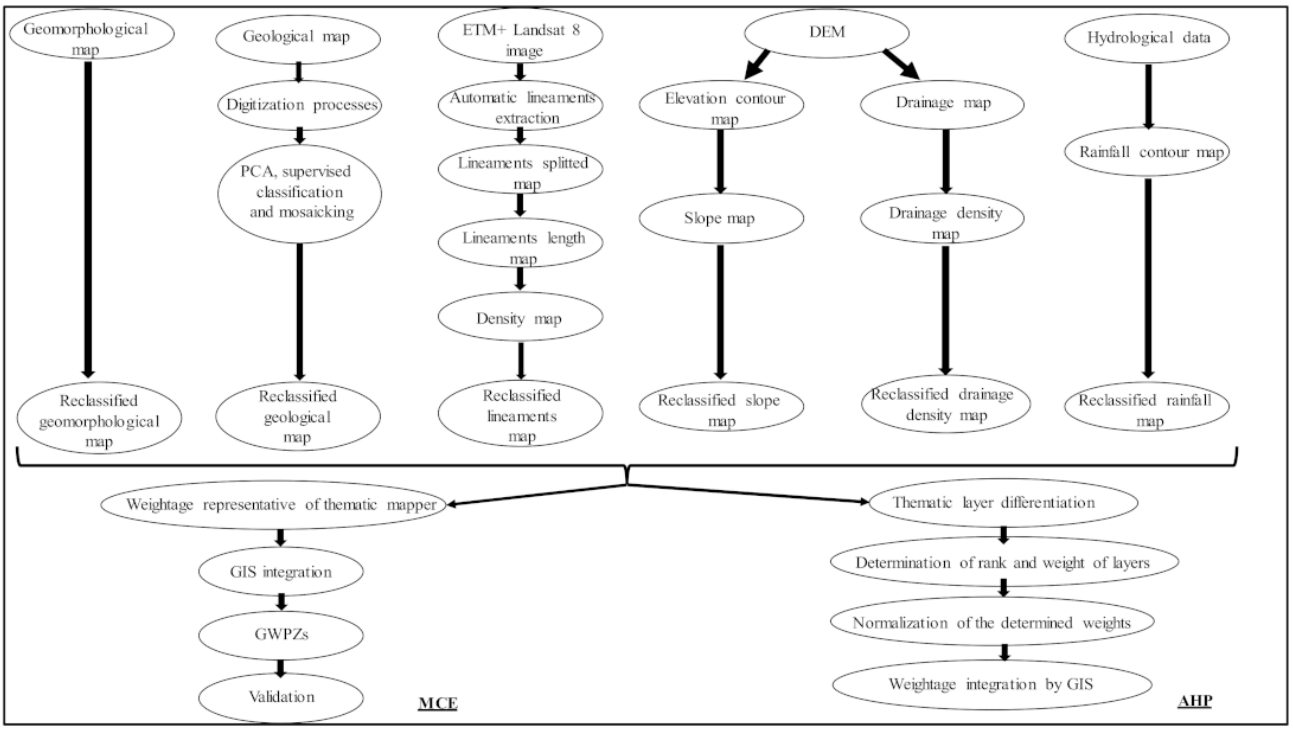

Figure 5. Methodology flow chart for the present study MCE and AHP techniques.

3. Results and Discussions

Thematic maps of geomorphology, geology, lineaments density, slope, drainage density, and rainfall were supervised to each other to produce the aquifer potentiality map. These geological, hydrological, and hydrogeochemical parameters contributed mainly to aquifer recharge. The stream network reflects the aquifer storage and surface runoff, while the lineaments represent the secondary conduits for rainfall leakage. The geological formation indicates the exposed sediments percolation capacity. The slope influences the runoff infiltration rate based on the surface water velocity. The input layers were ranked numerically. The ranked layers are determined based on their contribution to groundwater recharge. Each layer was divided into classes, which reflect the control on aquifer potentiality. All the weighted layers were integrated through GIS and produced groundwater potential maps [8,17,39].

3.1. Groundwater Potential Parameters

3.1.1. Rainfall

The arid climate and low precipitation are considered to be effective input recharge parameters for aquifers. Annual rainfall between 1965 and 2012 was collected at three sites (Qena, Safaga, and El Qusier). The geographic distribution and intensity of rainfall were analyzed using the isohyet method (ArcMap 10.2.2). Figure 6a shows the increase in rainfall was in the Safaga area (av. 4.9–5.7 mm/y). The resulting map (Figure 6b) shows five classes in which the potential (high recharge of groundwater) increases by category (high precipitation). Although rainfall was typically light, it may increase and reach heavy levels later. In this case, the precipitation increases or decrease trends are depicted in Figure 6. As a result, the contribution to aquifer potentiality was set, as shown in Figure 6.

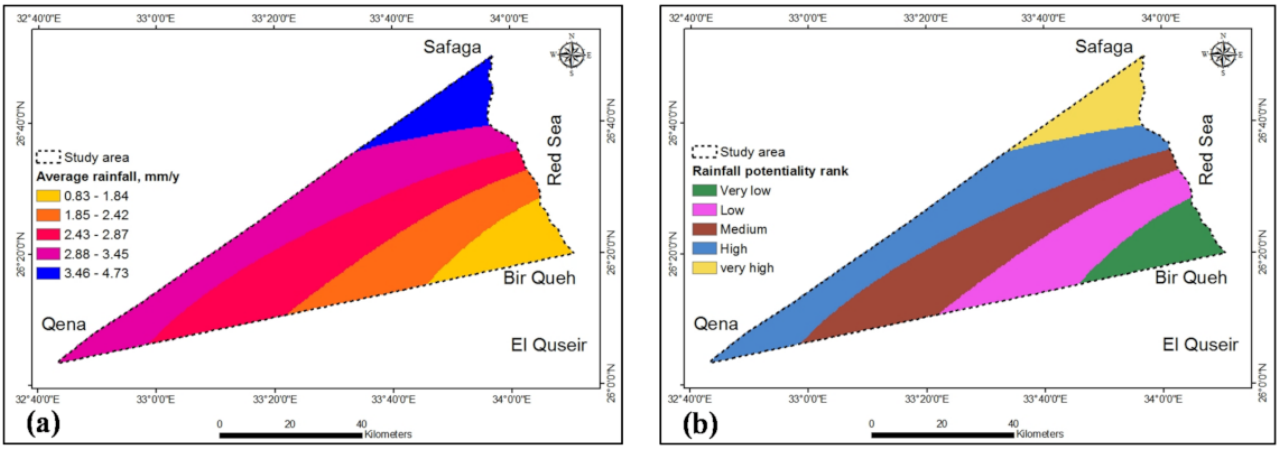

Figure 6. (**a**) Average annual rainfall and (**b**) reclassified rainfall of the study area.

3.1.2. Geology

The hydrogeological characteristics of the aquifer affect the recharge and storage of the aquifer. The high hydraulic conductivity improves the flow of groundwater, thereby increasing the recharge of the aquifer. Water leakage is affected by the hydrogeological properties of exposed aquifers. The supervised digital geologic map has been dissolved, and many grid codes in the GIS attribute table have been declined. The geological potential rank was established (between parenthesis) in Figure 2. The dissolved resultant map is subdivided into five geological areas based on geological potential rank (Figure 7). Based on lithological potentiality rank (contribution to recharge and storage of the aquifer), the study area was divided into five classes ranged from very low to very high aquifer potential (Figure 7). Higher weights were given to Nubian sandstone, which has higher permeability than carbonate and hard rocks.

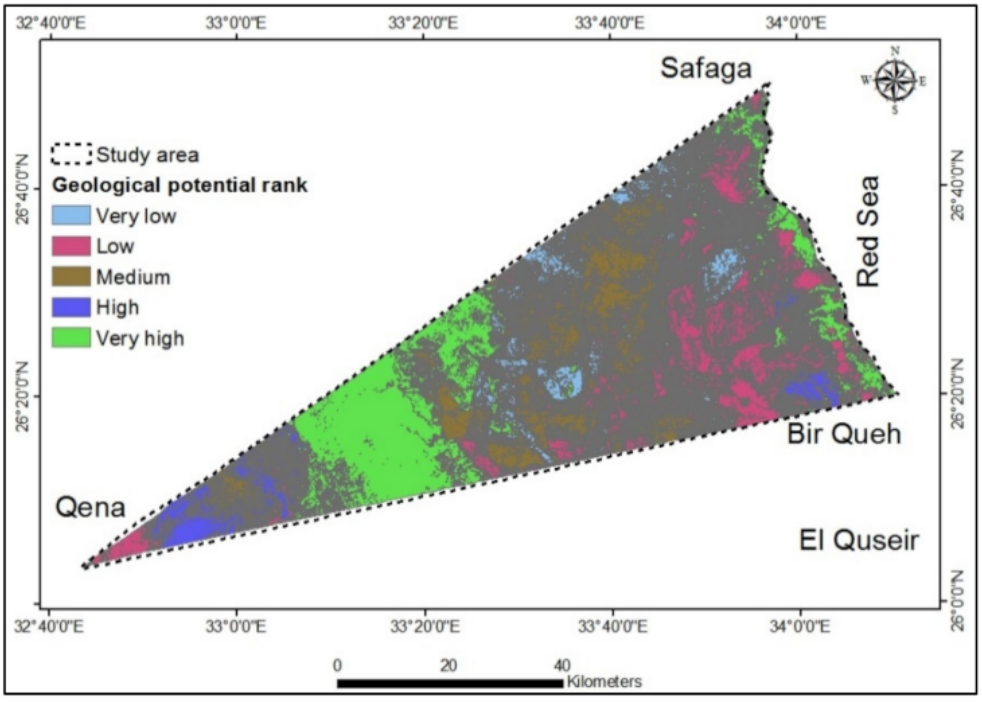

Figure 7. Dissolved geological areas based on potential rank.

3.1.3. Rock Fractures

Hydraulic conductivity is increased by the joint, fault, and fracture, resulting in increased downward leakage. These features were detected as linear features from the

satellite images. Fractures are exposed due to structural impact [40]. The identified fractures varied in length and directions. The structural sources might be the possible reason for traced linear (fractures) instead of anthropogenic influences, namely, roads, canals, and pipelines. The geological and non-geological linear characteristics match with a geologic map. The non-geologic lineaments were removed, and only the characteristics of geological lineaments features are observed (Figure 8a).

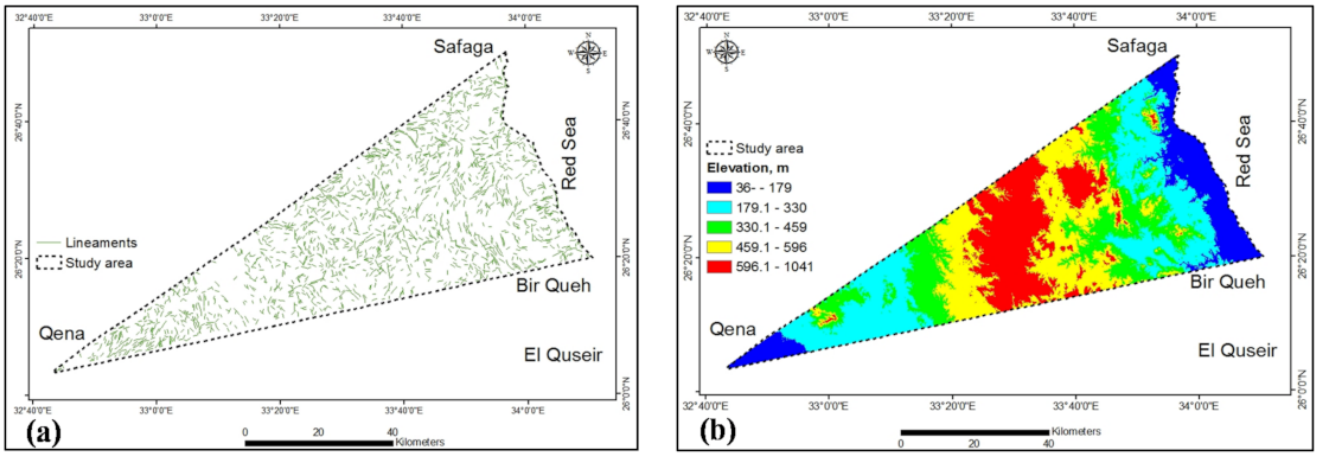

Figure 8. (**a**) Lineament and (**b**) topography distribution.

The study area is mainly covered by hard rocks, characterized by joint, fractures and faults systems, and rock weathering. The intense lineaments represent the main recharge for the aquifer. They are attributed to the greater number and larger and wider lengths, serving as conduits and better interconnections with other fractures [41]. The lineaments were extracted from the geological map and ETM+ 8 satellite image. They give us the most important data of the surface and sub-surface fractures systems, which affect aquifer storage [42,43]. The major fault runs in E-W, NE-SW, and NW-SE directions with variable concentration percentages (Figure 9). The lineaments length range (523.1–1001 m) was the highest number (1023), followed by the range 1001–1500 m, which counted 722 lineaments (Table 1).

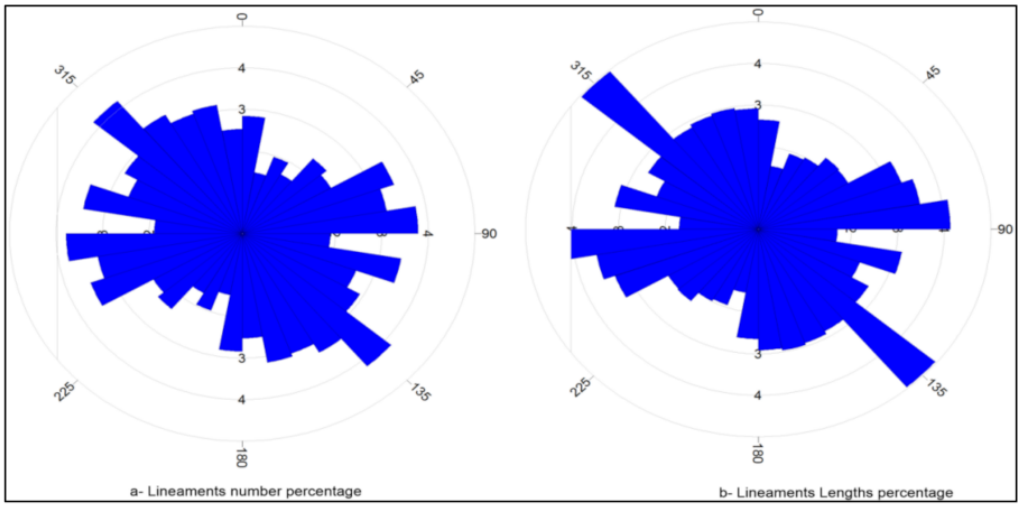

Figure 9. Rose diagrams of the lineaments.

Table 1. Ranges of lineaments length.

	Ranges of Lineaments Length (m)						
	3.6–523	**523.1–1001**	**1001–1500**	**1500–2003**	**2003–2571**	**2571–2925**	**3870.5**
Count:	913	1023	722	119	29	9	1
Minimum:	3.6	502.9	1001.3	1500.3	2003.1	2571.1	-
Maximum:	502.9	1001.3	1500	2003.1	2571.1	2925.3	-
Sum:	334,356.1	786,459	846,725.1	200,890.4	64,063.7	24,612	3870.5
Mean:	366.2	768.8	1172.7	1688.2	2209.1	2734.7	-
Standard Deviation:	99.3	175.7	128.2	142.2	147.8	128.9	-
Total lineaments lengths = 2,260,976.8 m							

The total lineaments lengths equal 2261 km. The study area showed 6th stream orders with total stream lengths of 5108 km (Table 2). The 1st order was the longest stream order, while the 6th was the shortest (Table 2).

Table 2. Lengths of the stream orders.

	Lengths of Orders (m)					
	1st Order	**2nd Order**	**3rd Order**	**4th Order**	**5th Order**	**6th Order**
Count:	2859	1301	747	324	166	73
Minimum:	4.6	57.3	44	44	124.5	44
Maximum:	9999.5	5301.7	5040.5	6964.8	2433.9	3721.4
Sum:	2,747,627.2	1,223,748	662,852.6	288,390.6	128,068.7	57,225.9
Mean:	961	940.6	887.4	890.1	771.5	783.9
Standard Deviation:	810.8	748	698.6	773.6	533.7	622
Total stream lengths = 5,107,912.9 m						

The density of the lineaments was divided into five categories ranging from very low density to very high density (Figure 10a). High to very high lineament density was excellent for the aquifer recharge, leakage, and potentiality. The lineaments density ranged from 0–1.3 km/km^2 (Figure 10a). The reclassified lineament density map was divided into five classes, which varied from very high potential (very high lineaments density) to very low potential rank (very low lineament density) (Figure 10b). The maximum potential of groundwater is consistent with the highest classes.

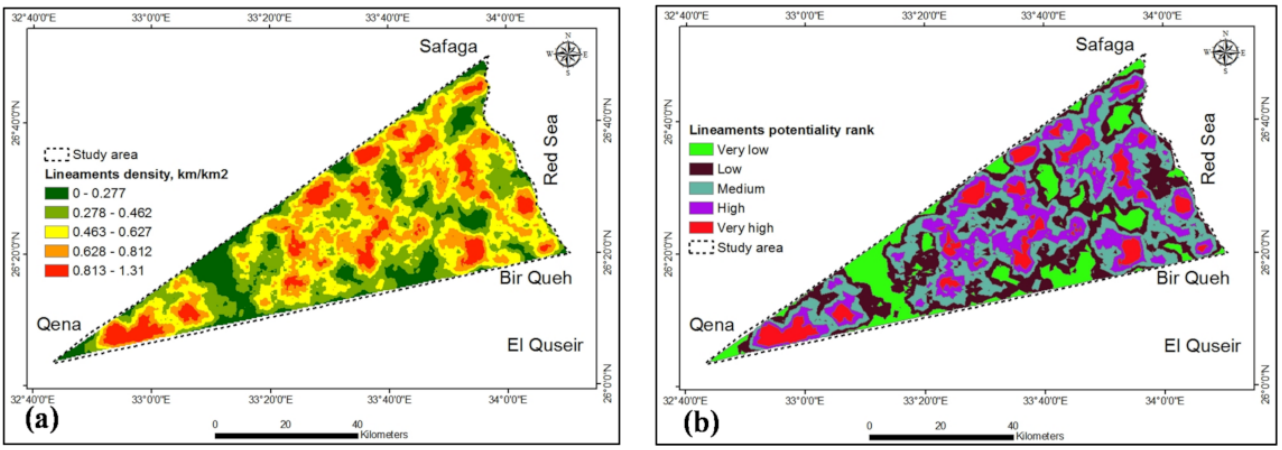

Figure 10. (**a**) Lineaments density and (**b**) reclassified lineaments density of the study area.

3.1.4. Slope

The slope of the land affects the surface runoff at different infiltration rates according to the topography, which in turn affects the recharge of the aquifer [44]. A low velocity of surface runoff characterizes a gentle slope; it is suitable for water leakage and promotes recharge of the aquifer. On the other hand, rapid runoff is detected in steep slopes, and thus there is no or less chance of infiltration and recharge of the aquifer. The ground elevation ranged from −36–1041 m, and the highest elevation was in the central part (see Figure 8b). The slope of the land was inversely proportional to the runoff infiltration. The slope ranged from 0–48.3° (Figure 11a), estimated by the digital elevation model SRTM (DEM). The lowest elevation was in the triangle head and base, while the high and fluctuated elevation was in the center (see Figure 8b). The undulating terrain impacts slope values [45]. The slope map was classified into five classes (very low potential to very high potential), which corresponded to slope ranges (38.61–48.25 to 0–9.65), respectively (Figure 11a,b). The ranking interval from low to steep slopes is based on the contribution rate to the aquifer recharge. Most of the wells are installed in wadis and far from hard rocks, which constitute the steep slope. Higher weights are assigned to a relatively low slope due to the higher recharging capacity. Five classes have been identified for reclassifying slopes (Figure 11b); the groundwater potential was highest in the lowest slopes.

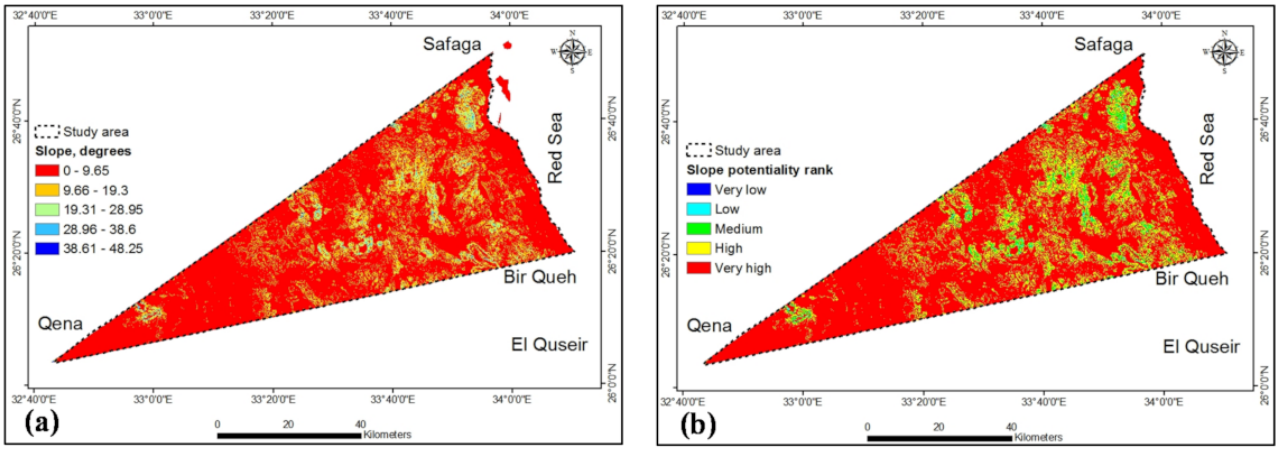

Figure 11. (**a**) Slope and (**b**) reclassified slope of the study area.

3.1.5. Drainage Density

This drainage map was prepared using SRTM-DEM 90 m resolution data in ArcGIS using the spatial analyst tool, and the method of stream ordering is according to Strahler (Figure 12). According to [46], stream order increases when streams of the same order intersect. Therefore, the intersection of a 1st-order and a 2nd-order link will remain a 2nd-order link rather than create a 3rd-order link. Drainage density was calculated by Horton's method [47] and equal the stream's total length divided by the catchment area (km/km^2). The reduction in groundwater recharge is related to the dense drainage pattern. The low drainage density is associated with the high recharge of the aquifer. The morphometric investigation of drainage basins reflects the hydrogeological conditions. The exposed geology influences the texture, composition, watershed density, and leakage -runoff relationships [41]. The flow channels (Figure 12) are extracted from the SRTM data elevation and have a 6th order. The geology, hard rock types, structural joints, fractures, and faults (linear lines) influence the distribution of flow channels.

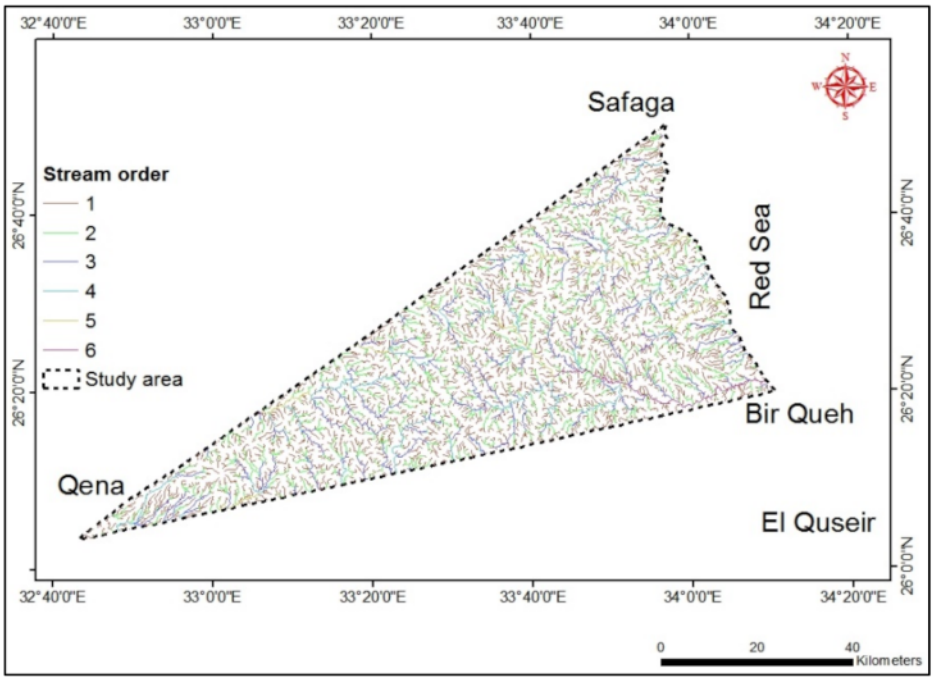

Figure 12. Drainage density map of the study area.

Drainage intensity was estimated from the SRTM map; it ranged from 3–651 km/km^2 (Figure 13a). It reclassified into five classes from very low to very high potential (Figure 13b), depending on its effect on the rate of water seepage. The categories of drainage density varied from very low to very high potential rank, so the smaller the drainage density, the greater the seepage into the aquifer, and vice versa.

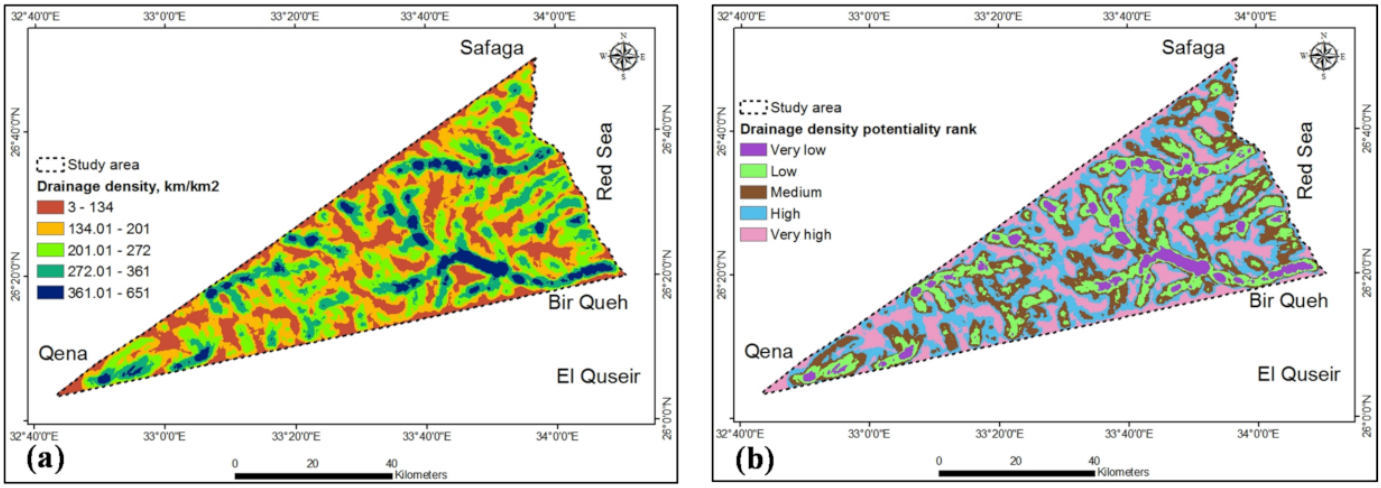

Figure 13. (**a**) Drainage density map and (**b**) reclassified drainage density map of the study area.

3.1.6. Geomorphology

It represents the most critical parameter for hydrogeological evaluation. Geology, geomorphology, and structures influence the aquifer potential and recharge [47]. The geomorphology is distinguished into four units (Figure 14a). The first was structural plains, which mainly covered sandstone. It is the highest weight and rank (Figure 14b). The second was the structural plateau and ridges, which occupy the hard rocks and flat carbonate sediments (main cover in the Eastern Desert). It follows the structural plains in weight and rank (Table 1, Tables 4 and 5). The third was basement ridge, which constitutes fractured

hard igneous and metamorphic rocks and has an average elevation of about 1000 m above mean sea level. The fourth was coastal plains, underlain mainly by beach sand and lagoonal mud. The groundwater salinity in coastal plains is very high due to seawater intrusion and low thickness. It is the lowest weight and rank (Figure 14b). The hydro-geomorphological units were scanned, rectified and digitized in the GIS model. This section may be divided by subheadings. It should provide a concise and precise description of the experimental results, their interpretation, as well as the experimental conclusions that can be drawn.

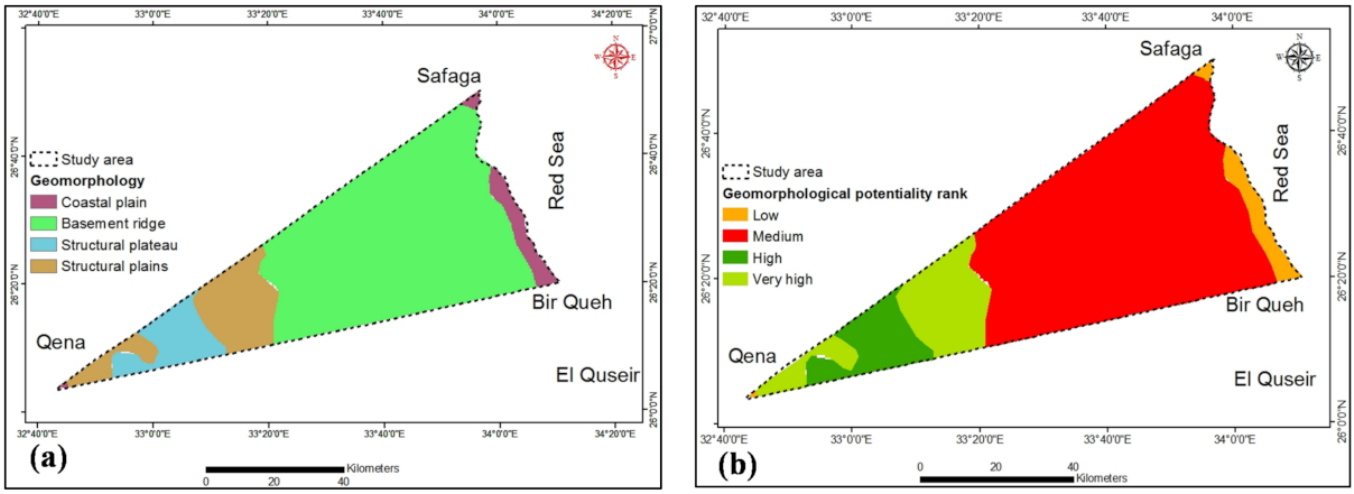

Figure 14. (**a**) Morphological structures and (**b**) reclassified morphological structures of the study area.

3.2. GWPZs Mapping

3.2.1. GWPZs by MCE and Its Validation

The MCE technique was identified by [17]. An aquifer potential map was extracted from various geological, hydrogeological, and hydrological thematic maps and is very important for agricultural, domestic, and industrial applications. Weights were given for each variable according to the contribution to groundwater recharge (Table S1). These thematic maps were integrated through a GIS model to predict the most promising map of aquifer potential. The map rank is transformed into map weight by dividing the map rank from the sum of parameters ranks (Table S1). The map categories assigned different class ranges, which ranged from 1 (lowest favorable) to 5 (highest favorable), except morphological structures, which ranged from 1–4 (Table S1). The rank of each class has been divided by the total cluster values of the layer classes to calculate the capability values (CVs) (Table S1). These CVs are multiplied by the weight of the relevant probability layer in each thematic layer to compute the groundwater probability map (Figure 15). It is calculated mathematically using the ArcGIS raster analysis as follows:

$$GWP = \sum Wt. * CV \quad (1)$$

where, GWP = groundwater potential, Wt. = map weight, and CV = capability value.

GWP = ∑ morphological structures, geology, lineaments density, slope, drainage density, and rainfall.

The aquifer potential map has been classified into five classes ranging from very low to very high probability (Figure 15). The maximum groundwater recharge was located in the central and western parts of the study area (Figure 15). The high to very potential zones include 1467 km^2 (36%) of the area (Table 3). They are collected in approximately one body of enclosed area, not separate. They are distinguished by high lineaments, low drainage density, suitable geology (sandstone), and gentle slope. The enclosed area needs much more study to concentrate more on aquifer promising areas and excellent well pumping. The low to very low potential zones constitutes 1752 km^2 (43%) (Table 3) and are separated randomly in the eastern part of the study area (Figure 15). High drainage density, low

lineaments density, steep slope, and hard rocks characterize them. The spotted northern rim of the eastern part was distinguished by high to very high aquifer potential.

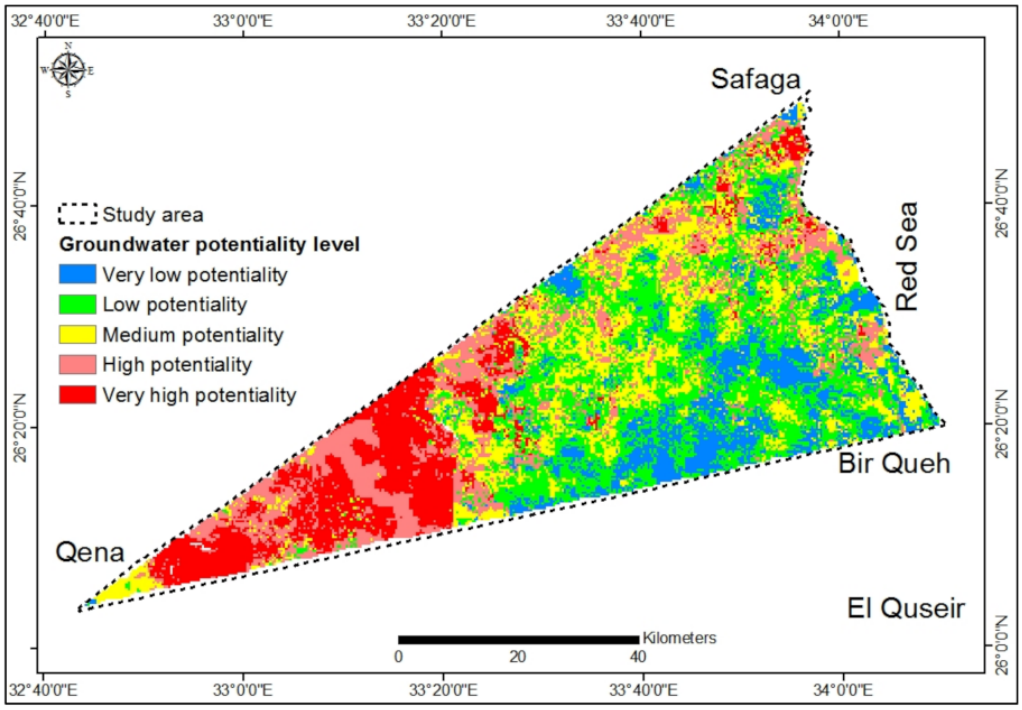

Figure 15. GWPZs map of the study area by MCE technique.

Table 3. Percentage of GWPZs by MCE and AHP technique.

	MCE		AHP	
GWPZs	**Area (km^2)**	**Area (%)**	**Area (km^2)**	**Area (%)**
Very low	580.3	14.3	259.7	6.1
Low	1172.3	29	1138.6	26.9
Medium	825.7	20.4	1479.3	34.9
High	780.7	19.3	693.4	16.4
Very high	686.6	17	667.2	15.7

The validation approach is achieved by matching the measured aquifer TDS in the borehole and correlate it with GWPZs. The validation outputs show that the well with good water quality are mostly located in high to very high potential zones. The TDS concentration of meta-sediments, and Duwi aquifers are located in high potential zones. The low TDS concentration of both aquifers (suitable for irrigation purposes) (Table 4) match with high potential zones (Figure 16a), which reflect good outputs and high accuracy. The high TDS concentration of limestone aquifer (unsuitable for irrigation) (Table 4) is represented in low to very low potential zones (Figure 16a), which indicate excellent outputs.

The TDS concentration of the basement aquifer was 801 ppm and 1232 ppm (Table 4), which occupied the very high potential zone (Figure 16b), which encourage decision-makers to increase the detailed investigation. The high to very high TDS concentration of the basement aquifer covers the medium potential zone, except for one sample of 5163 ppm, which reflect mismatch and poor outputs (Figure 16b). The TDS concentration of the basement aquifer ranged from 8226 ppm −13209 ppm coincides with medium potential zones, which are considered acceptable outputs. The high TDS concentration of the aquifers (Figure 17) correlated with medium to very low potential, which indicates good accuracy of the applied technique (Table 5). The exception was hand-dug of TDS concentration 337

ppm and located in the low potential zone, reflecting poor outputs. The dug well may dry up in summer, and the drying fluctuation levels changes periodically.

Table 4. First validation of GWPZs with TDS concentration based on aquifer type.

Aquifer Type	TDS (ppm)	MCE Method	AHP Method
Metasediments	744	High potential	Medium Potential
Quaternary	1580	Outside	Outside
Duwi	1399	High potential	Low potential
Limestone	4141	Low potential	Very low potential
Limestone	7565	Very low potential	Very low potential
Limestone	9062	Outside	Outside
Basement	805	Outside	Outside
Basement	4430	Outside	Outside
Basement	9345	Outside	Outside
Basement	801	Very high potential	High potential
Basement	1232	Very high potential	High potential
Basement	5163	High potential	Medium Potential
Basement	13,209	Medium potential	Medium Potential
Basement	8226	Medium potential	Medium Potential
Basement	10,130	Medium potential	Medium Potential

Table 5. Second validation of GWPZs with TDS concentration based on borehole type.

Borehole Type	TDS (ppm)	MCE Method	AHP Method
Drilled	2827.9	Medium potential	Medium potential
Shaft	11,693.4	Low potential	Low potential
Shaft	9313.89	Low potential	Very low potential
Hand dug	11,368.2	Very low potential	Very low potential
Hand dug	10,967.9	Medium potential	Medium potential
Hand dug	5040.49	Medium potential	Medium potential
Drilled	14,424.2	Medium potential	Very low potential
Hand dug	337.07	Low potential	Low potential
Drilled	6986.9	Low potential	Medium potential
Drilled	2068	Medium potential	Medium potential
Hand dug	371	High potential	High potential

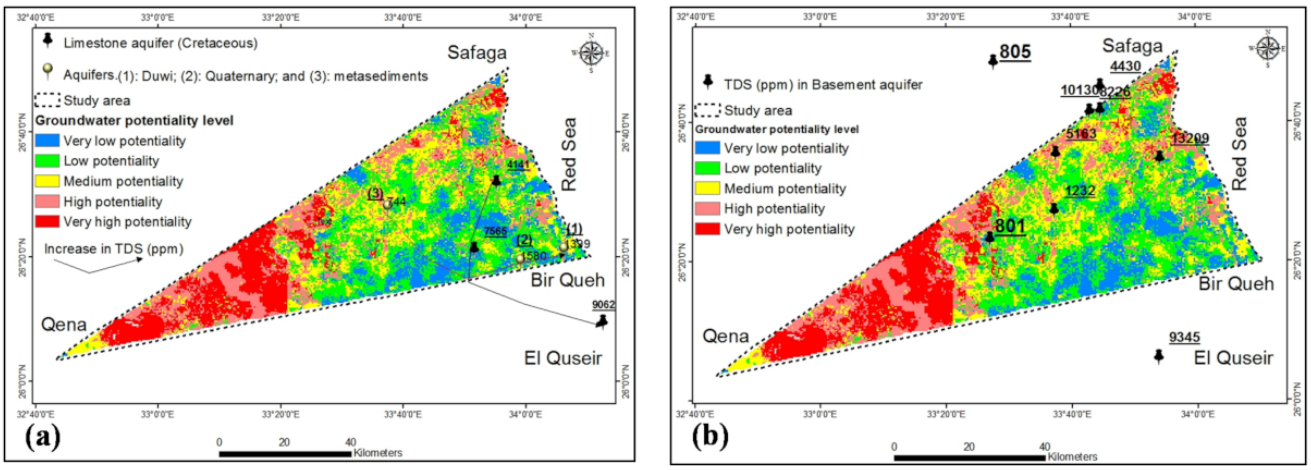

Figure 16. First validation of the GWPZs with aquifers TDS concentration by MCE technique. High potential zones (**a**); very high potential zone (**b**).

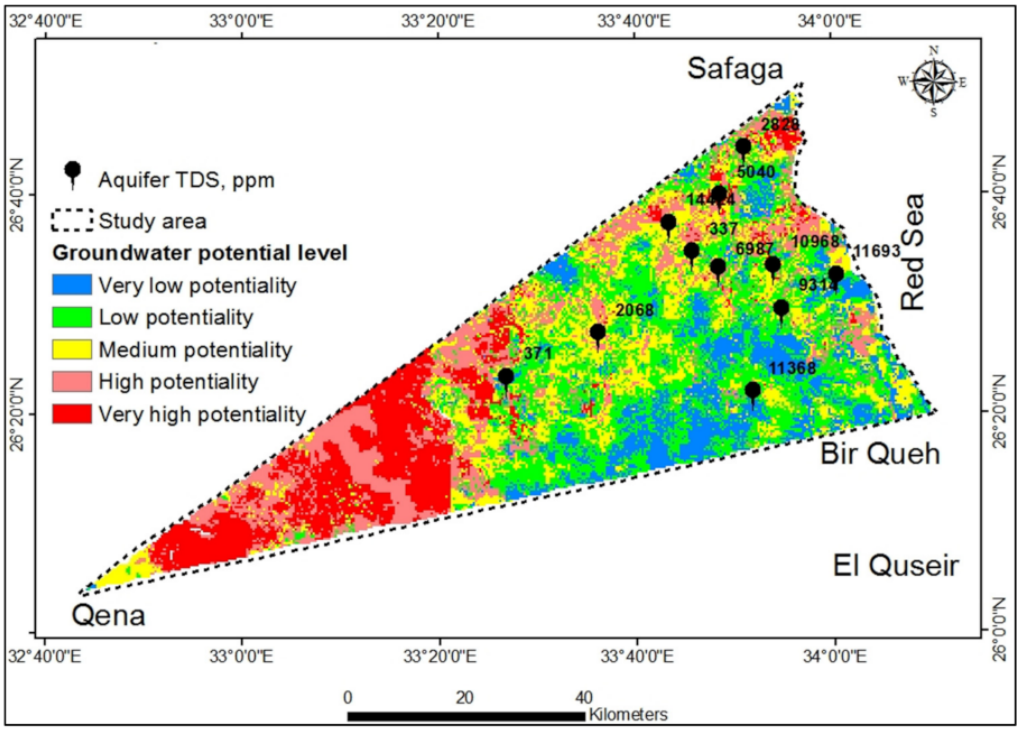

Figure 17. Second validation of the GWPZs with aquifers TDS concentration by MCE technique.

3.2.2. GWPZs by AHP and Its Validation

The AHP technique was famous for extracting aquifer potentiality zones [24]. They overlay six thematic maps (morphological structures, geology, lineaments density, slope, drainage density, and rainfall), influencing aquifer potentiality and recharge.

The parameters weight was determined from his contribution to aquifer recharge and groundwater occurrences. The aquifer potential levels were assigned by overlaying six thematic layers by the weighted process. The GWPZs were evaluated by integrating all the spatial layers using a weighted overlay approach. The parameters were reclassified to 1–5 rank, except morphological structures of 1–4, whereas 1 a was very low potential zone and 5 was a very high potential zone. The weights of the six parameters evaluated by a pair-wise comparison matrix depend on AHP (Table 6 and Table S2).

Table 6. Normalized Pairwise comparison matrix (six layers) assessed in AHP, depends upon contribution to aquifer recharge.

Parameters	Geomorphology	Geology	Lineaments	Slope	Drainage	Rainfall	Weight
Geomorphology	6	5	4	3	2	1	0.41
Geology	6/2	5/2	4/2	3/2	2/2	1/2	0.2
Lineaments	6/3	5/3	4/3	3/3	2/3	1/3	0.14
Slope	6/4	5/4	4/4	3/4	2/4	1/4	0.1
Drainage	6/5	5/5	4/5	3/5	2/5	1/5	0.082
Rainfall	6/6	5/6	4/6	3/6	2/6	1/6	0.068
Total							1

The ranks were evaluated based on field visits, experiences in hydrogeology and hydrology of the area under investigation, previous studies, and decision-making opinions. The hydro-geomorphological parameter was the highest weight, followed by geology, lineaments, slope, drainage and ends by lowest weight (rainfall) (Table 6 and Table S2). Then, the individual ranks were assigned for sub-parameter [47–49]. All six parameter

layers were incorporated with weightage, which was determined by multiplying the weight with a rank of the sub-variable parameter (Table S2).

$$GWPZ = \sum Wt. * Rank \text{ (for six layers)} \quad (2)$$

Wt.: weight of the thematic layer; Rank: contribution rate for aquifer potentiality of the sub variable parameter.

The union option in GIS calculates the aquifer potentiality zones. The maximum values for the prospect map were the very high potential, while the lowest values represent the very low potential. Hydro-geomorphology, geology, lineaments, slope, drainage, and rainfall were integrated with GIS to delineate the aquifer potential zones, ranging from very low to very high potential (Figure 18 and Table S2). The low and very low potential zones were randomly distributed in the eastern part of the study area (Figure 18). They represent 1398 km^2 (33%) and concentrate mainly in the mountainous areas (Table 3). They are distinguished by steep slope, high drainage density, low lineaments density, and mainly hard rocks cover. The high to very high potential zones have 1360 km^2 (32%) (Table 3) and are mainly included in the central and western part of the study area (Figure 18). They have been characterized by a gentle slope, low drainage density, good geology (mainly sandstone), and high lineaments density. They concentrated in one body area and not separate areas.

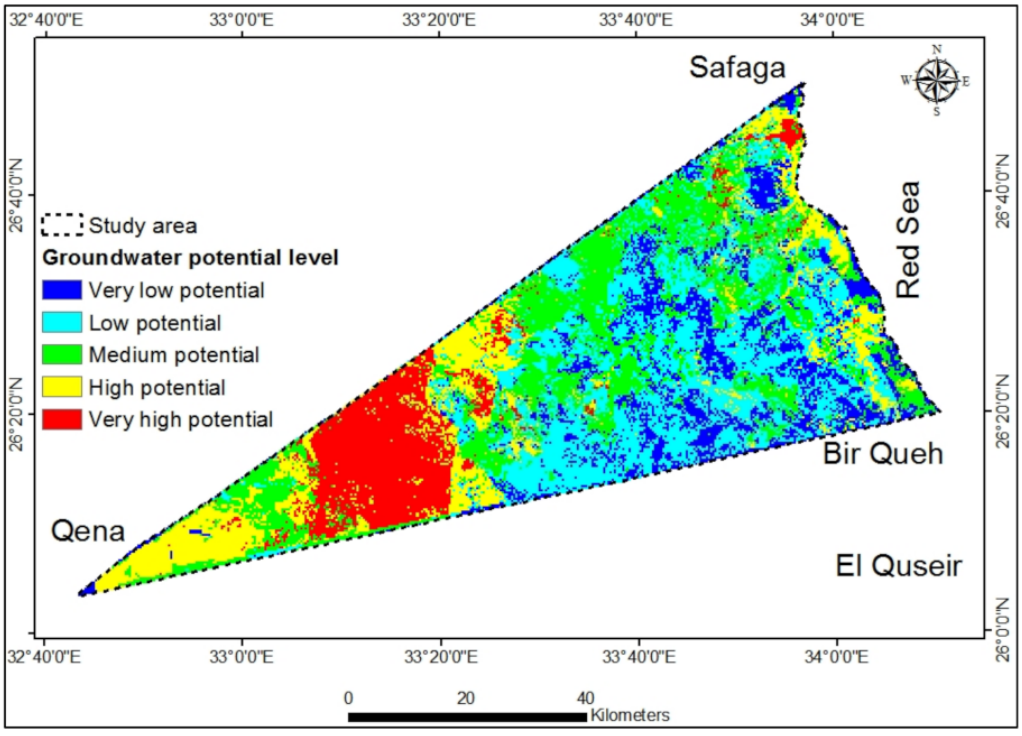

Figure 18. GWPZs map of the study area by AHP technique.

The TDS concentration of 744 ppm, 1399 ppm, 4141 ppm, and 7565 ppm (see Table 4) coincide with medium, low potential, very low potential, and very low potential, respectively (Figure 19a). They indicate a good match between GWPZs extracted and groundwater TDS concentration. They encourage us to investigate these boreholes more to add agricultural and drinking wells for investment and move the dwellers from the Nile Delta area (Qena) into the desert. The TDS content of the basement aquifer of 801 and 1232 ppm (Figure 19b) was included in the high potential zone, while the rest high TDS concentration was in the medium potential zone. The high TDS concentration of the aquifers is located in medium to very low potential zones (Figure 20), which indicate good accuracy of the applied technique (Table 5). They indicate a good match and needs much more investi-

gation and analysis. This good match between GWPZs and TDS aquifer concentration reflects the high accuracy of the AHP evaluation and encourage decision-makers for future investigation. The outputs identified by this AHP technique are characterized by better accuracy in aquifer potential zones through good validation.

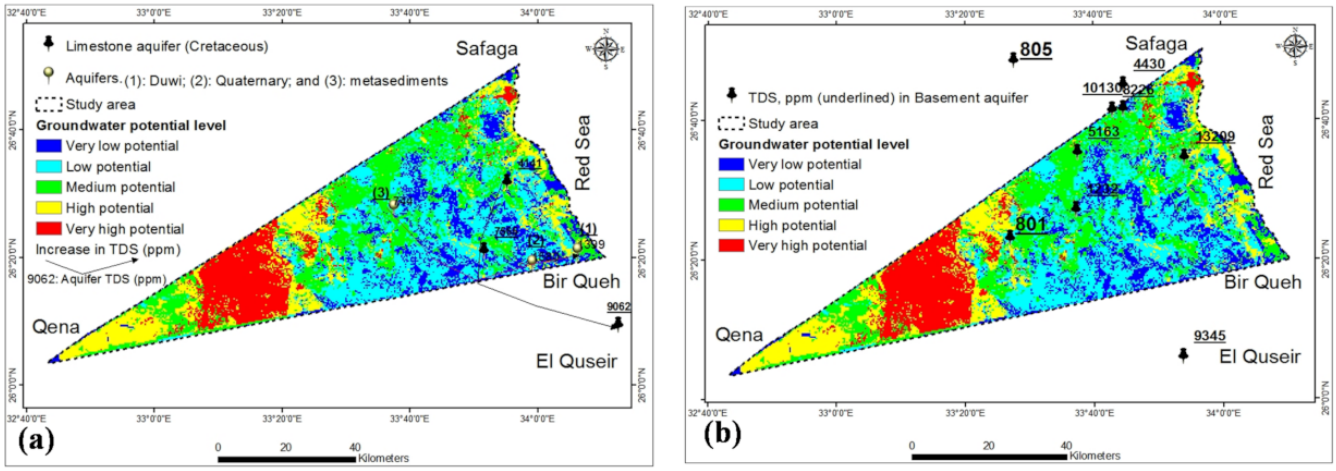

Figure 19. First validation of GWPZs with successful wells by AHP technique. Low potential, very low potential, and very low potential (**a**); aquifer of 801 and 1232 ppm (**b**).

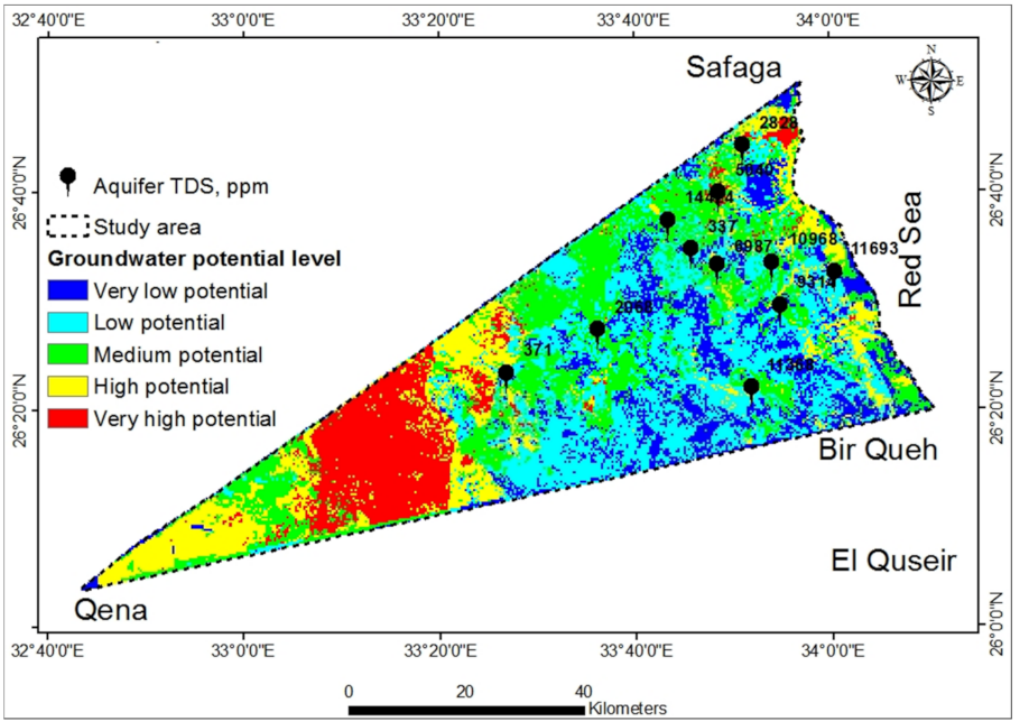

Figure 20. Second validation of GWPZs with successful wells by AHP technique.

3.3. Comparison between MCE and AHP Techniques

The GWPZs areas do not differ significantly between MCE and AHP in accuracy and percentage. Both techniques show that most of the central and western parts of the study area are high to very high potential. The validation of both techniques was mainly good, which reflect good outputs and high accuracy. They encourage the decision-makers to move the dwellers from Qena (high population density) to desert areas (excellent potential zones). It declines the pressure on Nile Delta areas and distributes the population more

or less equally through Egypt. The groundwater flows from the two highest elevations toward the lowest elevation.

The first highest elevation refers to the central area (recharge 1), which flows into the western part of the study area, approximately one discharge area (Figure 21). Therefore, the collection of the groundwater volumes through the western part was accomplished by the hydrogeological conditions of the area. Accordingly, it is considered the best promising area for aquifer exploration and exploitation, as stated by the two techniques (MCE and AHP). Recharge 1 also flows in the eastern part. The second highest elevations refer to the northeastern part (recharge 2), which flows into the northeast, east, and southeast, but in separate discharge areas (Figure 21). The groundwater volumes collected from the aquifer flow was high in 1st recharge zone than 2nd recharge zone.

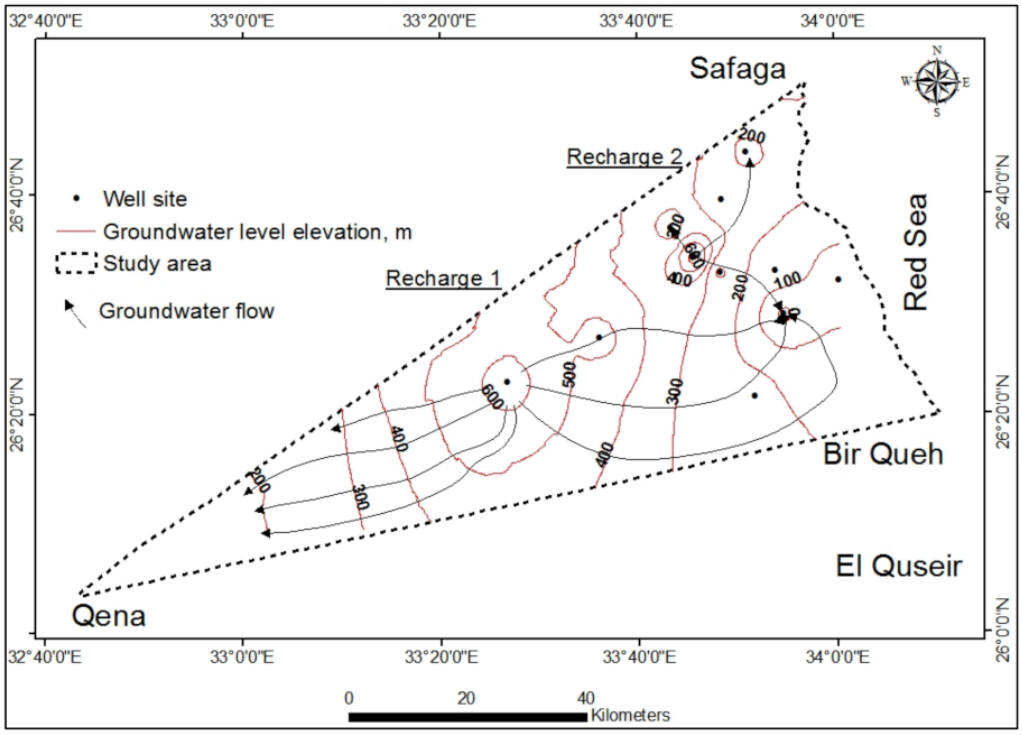

Figure 21. Groundwater flow map of the study area.

4. Conclusions

This research aims to expand agricultural land and population migration outside the Nile basin. Groundwater resources are limited, and precipitation infiltration into the aquifer is dependent on an open fracture system. Conduit channels are medium to low in metamorphic and igneous rocks, representing the majority of exposed rocks. GIS technique constructs and overlaps various raster layers, including morphological structures, geology, lineaments density, slope, drainage density, and rainfall. They are critical in the storage and transportation of groundwater.

The GWPZs were created using the AHP and MCE methods and classified into five potential zones: very low, low, medium, high, and very high. Very low and low aquifer potential zones are distributed randomly throughout the study area and are primarily exposed by hard rocks. Zones with high to very high potential are concentrated in an enclosed area in the central and western parts. The GWPZ areas and geospatial sites are not significantly different between the AHP and MCE methods. The GWPZs were validated using aquifer TDS concentration and groundwater flow, and both techniques showed good accuracy. It ensures that RS and GIS can identify the best areas for agriculture, development, and residential sites.

The GWPZs map provides decision-makers with the best aquifer resource planning and management to improve the irrigation industry and encourage Bedouins and Nile River residents to relocate to the deserts. Further research on the eastern desert lands parallel to the Nile will attract people from the Nile to the desert areas, thereby evenly distributing Egypt's population. The most promising research outcomes are land use management, aquifer resource planning, usage, and high income/capita.

Supplementary Materials: The following supporting information can be downloaded at: https://www.mdpi.com/article/10.3390/w14071041/s1, Table S1: Weight and CVs of thematic maps by MCE techniques; Table S2: Weights determined for geological, hydrogeological and hydrological parameters for AHP.

Author Contributions: Conceptualization, M.E. and M.Y.A.K.; methodology, M.E.; software, M.E.; validation, M.E.; writing—original draft preparation, M.Y.A.K. and M.E.; writing—review and editing, M.Y.A.K. and F.T. All authors have read and agreed to the published version of the manuscript.

Funding: This project was funded by the Deanship of Scientific Research (DSR) at King Abdulaziz University Jeddah, under grant no. G: 294-145-1442. The authors, therefore, acknowledge with thanks the DSR for technical and financial support.

Institutional Review Board Statement: Not applicable.

Informed Consent Statement: Not applicable.

Data Availability Statement: Not Applicable.

Conflicts of Interest: The authors declare no conflict of interest.

References

1. Gaber, A.; Koch, M.; Griesh, M.H.; Sato, M. SAR Remote sensing of buried faults: Implications for groundwater exploration in the Western Desert of Egypt. *Sens. Imaging Int. J.* **2011**, *12*, 133–151. [CrossRef]
2. IPCC. Climate Change 2007: The Physical Science Basis. In *Contribution of Working Group I to the Fourth Assessment Report of the Intergovernmental Panel on Climate Change*; Solomon, S., Qin, D., Manning, M., Chen, Z., Marquis, M., Averyt, K.B., Tignor, M., Miller, H.L., Eds.; Cambridge University Press: Cambridge, UK; New York, NY, USA, 2007; 996p.
3. Gheith, H.; Sultan, M. Construction of a hydrologic model for estimating Wadi runoff and groundwater recharge in the Eastern Desert, Egypt. *J. Hydrol.* **2002**, *263*, 36–55. [CrossRef]
4. Mosaad, S. Geomorphologic and geologic overview for water resources development: Kharit basin, Eastern Desert, Egypt. *J. Afr. Earth Sci.* **2017**, *134*, 56–72. [CrossRef]
5. Naim, G. *Floods of Upper Egypt Governorates*; Egyptian Geological Survey and Mining Authority: Cairo, Egypt, 1995.
6. Agarwal, R.; Garg, P. Remote sensing and GIS based groundwater potential & recharge zones mapping using multi-criteria decision making technique. *Water Resour. Manag.* **2016**, *30*, 243–260.
7. Sander, P.; Minor, T.B.; Chesley, M.M. Ground-water exploration based on lineament analysis and reproducibility tests. *Groundwater* **1997**, *35*, 888–894. [CrossRef]
8. Eastman, J.R. *Multi-Criteria Evaluation and Geographical Informationn Systems*; Longley, P.A., Goodchild, M.F., Magurie, D.J., Rhind, D.W., Eds.; John Wiley and Sons: New York, NY, USA, 1996; Volume 1, pp. 493–502.
9. Taheri, A.; Zare, M. Groundwater artificial recharge assessment in Kangavar Basin, a semi-arid region in the western part of Iran. *Afr. J. Agric. Res.* **2011**, *6*, 4370–4384.
10. Chowdhury, A.; Jha, M.K.; Chowdary, V.M. Delineation of groundwater recharge zones and identification of artificial recharge sites in West Medinipur district, West Bengal, using RS, GIS and MCDM techniques. *Environ. Earth Sci.* **2010**, *59*, 1209–1222. [CrossRef]
11. Meshram, K.S. Effect of Artificial Recharge Structures on Ground Water Availability in Semi-critical Area in Chhattisgarh. Ph.D. Thesis, Indira Gandhi KrishiVishwavidyalaya, Raipur, India, 2010; pp. 4–23.
12. Samson, S.; Elangovan, K. Delineation of groundwater recharge potential zones in Namakkal District, Tamilnadu, India using remote sensing and GIS. *J. Indian Soc. Remote Sens.* **2015**, *43*, 769–778. [CrossRef]
13. Deepika, B.; Avinash, K.; Jayappa, K.S. Integration of hydrological factors and demarcation of groundwater prospect zones: Insights from remote sensing and GIS techniques. *Environ. Earth Sci.* **2013**, *70*, 1319–1338. [CrossRef]
14. Deepa, S.; Venkateswaran, S.; Ayyandurai, R.; Kannan, R.; Prabhu, M.V. Groundwater recharge potential zones mapping in upper Manimuktha Sub basin Vellarriver Tamil Nadu India using GIS and remote sensing techniques. *Modeling Earth Syst. Environ.* **2016**, *2*, 137. [CrossRef]

15. Machiwal, D.; Rangi, N.; Sharma, A. Integrated knowledge- and data-driven approaches for groundwater potential zoning using GIS and multi-criteria decision making techniques on hard-rock terrain of Ahar catchment, Rajasthan, India. *Environ. Earth Sci.* **2015**, *73*, 1871–1892. [CrossRef]
16. El Mekki, O.A.; Laftouhi, N.-E. Combination of a geographical information system and remote sensing data to map groundwater recharge potential in arid to semi-arid areas: The Haouz Plain, Morocco. *Earth Sci. Inform.* **2016**, *9*, 465–479. [CrossRef]
17. Voogd, H. Multi-Ctiteria Evaluation for Urban and Regional Planning, Pion, London. *Water Resour. Manag.* **1983**, *24*, 921–939.
18. Todd, D.K.; Mays, L.W. *Groundwater Hydrology*, 3rd ed.; John Wiley & Sons: Hoboken, NJ, USA, 2013.
19. Adiat, K.A.N.; Nawawi, M.N.M.; Abdullah, K. Assessing the accuracy of GIS-based elementary multi-criteria decision analysis as a spatial prediction tool—a case of predicting potential zones of sustainable groundwater resources. *J. Hydrol.* **2012**, *440*, 75–89. [CrossRef]
20. Pradhan, R.M.; Guru, B.; Pradhan, B.; Biswal, T.K. Integrated multi-criteria analysis for groundwater potential mapping in Precambrian hard rock terranes (North Gujarat), India. *Hydrol. Sci. J.* **2021**, *66*, 961–978. [CrossRef]
21. Roy, S.; Hazra, S.; Chanda, A.; Das, S. Assessment of groundwater potential zones using multi-criteria decision-making technique: A micro-level case study from red and lateritic zone (RLZ) of West Bengal, India. *Sustain. Water Resour. Manag.* **2020**, *6*, 4. [CrossRef]
22. Jothibasu, A.; Anbazhagan, S. Modeling groundwater probability index in Ponnaiyar River basin of South India using analytic hierarchy process. *Model. Earth Syst. Environ.* **2016**, *2*, 109. [CrossRef]
23. Khan, M.Y.A.; ElKashouty, M.; Subyani, A.M.; Tian, F.; Gusti, W. GIS and RS intelligence in delineating the groundwater potential zones in Arid Regions: A case study of southern Aseer, southwestern Saudi Arabia. *Appl. Water Sci.* **2022**, *12*, 3. [CrossRef]
24. Saaty, T.L. *The Analytic Hierarchy Process: Planning, Priority Setting, Resources Allocation*; McGraw: New York, NY, USA, 1980.
25. Abdalla, F. Mapping of groundwater prospective zones using remote sensing and GIS techniques: A case study from the Central Eastern Desert, Egypt. *J. Afr. Earth Sci.* **2012**, *70*, 8–17. [CrossRef]
26. Said, R. *The Geology of Egypt*; Elesvier Publication: Amsterdam, The Netherlands, 1962.
27. Said, R. *The Geology of Egypt*; Balkema, A.A., Ed.; Brookfield: Rotterdam, The Netherlands, 1990; p. 734.
28. El Ramly, I.M. *Final Report on Geomorphology, Hydrology Planning for Groundwater Resources and Reclamation in Lake Nasser Region and Its Environs*; Cen And Des Inst.: Cairo, Egypt, 1972; p. 603.
29. EGPC/Conoco. *Photogeological Interpretation Map, Scale (1: 100,000)*; CORALI: Cairo, Egypt, 1987.
30. Gomaa, M.A. Hydrogeological Studies between Quesir-Safagaarea, Eastern Desert, Egypt. Master's Thesis, Ain Shams Univ., Cairo, Egypt, 1992; p. 172.
31. ElKashouty, M. Watershed delineation and morphometric analysis using remote sensing and GIS mapping techniques in Qena-Safaga-BirQueh, Central Eastern Desert. *Int. J. Water Resour. Environ. Eng.* **2020**, *12*, 22–46.
32. El Shazly, E.M. The geology of the Egyptian region. In *The Ocean Basins and Margins*; Springer: Boston, MA, USA, 1977; pp. 379–444.
33. Gomaa, M.D.; Meraj, N.M.; Khaled, A.A. Assessment of several flood estimation methodologies in Makkah metropolitan area, Saudi Arabia. *Arab. J. Geosci.* **2013**, *6*, 985–993.
34. Moneim, A.A.A.; Seleem, E.M.; Zeid, S.A.; Samie, S.G.A.; Zaki, S.; Abu El-Fotoh, A. Hydrogeochemical characteristics and age dating of groundwater in the Quaternary and Nubian aquifer systems in Wadi Qena, Eastern Desert, Egypt. *Sustain. Water Resour. Manag.* **2015**, *1*, 213–232. [CrossRef]
35. Elbeih, S.F.; Belal, A.A.B.; Zaghloul, E.S.A. Hazards mitigation and natural resources evaluation around Sohag–Safaga highway, Eastern Desert, Egypt. *Egypt. J. Remote Sens. Space Sci.* **2011**, *14*, 15–28. [CrossRef]
36. Abdalla, F.A.; Khalifa, I.H. Effects of phosphate mining activity on groundwater quality at WadiQueh, Red Sea, Egypt. *Arab. J. Geosci.* **2013**, *6*, 1273–1282. [CrossRef]
37. Eastman, J.R.; Jin, W.; Kyem, A.K.; Toledano, J. Raster Procedures for Multi-Criteria/Multi-Objective Decisions. *Photogramm. Eng. Remote Sens.* **1995**, *61*, 539–547.
38. O'leary, D.W.; Friedman, J.D.; Pohn, H.A. Lineament, linear, lineation: Some proposed new standards for old terms. *Geol. Soc. Am. Bull.* **1976**, *87*, 1463–1469. [CrossRef]
39. Edet, A.E.; Okereke, C.S.; Teme, S.C.; Esu, E.O. Application of remote-sensing data to groundwater exploration: A case study of the Cross-River State, southeastern Nigeria. *Hydrogeol. J.* **1998**, *6*, 394–404. [CrossRef]
40. Pradeep, R. Remote sensing techniques to locate ground water potential zones in upper Urmil River Basin, District Chhatarpur—Central India. *J. Indian Soc. Remote Sens.* **1998**, *26*, 135–147.
41. Sreedhar, G. Mapping of groundwater potential zones in the Musi basin using remote sensing data and GIS. *Adv. Eng. Softw.* **2009**, *40*, 506–518.
42. Al Saud, M. Mapping potential areas for groundwater storage in WadiAurnah Basin, western Arabian Peninsula, using remote sensing and geographic information system techniques. *Hydrogeol. J.* **2010**, *18*, 1481–1495. [CrossRef]
43. Das, B.; Pal, S.C. Assessment of groundwater recharge and its potential zone identification in groundwater-stressed Goghat-I block of Hugli District, West Bengal, India. *Environ. Dev. Sustain.* **2020**, *22*, 5905–5923. [CrossRef]
44. Strahler, A.N. Quantitative geomorphology of drainage basins and channel networks. In *Handbook of Applied Hydrology*; Chow, V.T., Ed.; McGraw Hill Book Company: New York, NY, USA, 1964; pp. 4–11.
45. Horton, R.E. Drainage basin characteristics. *Trans. Am. Geophys. Union* **1932**, *13*, 348–352. [CrossRef]

46. Patra, S.; Mishra, P.; Mahapatra, S.C. Delineation of groundwater potential zone for sustainable development: A case study from Ganga Alluvial Plain covering Hooghly district of India using remote sensing, geographic information system and analytic hierarchy process. *J. Clean. Prod.* **2018**, *172*, 2485–2502. [CrossRef]
47. Butler, M.; Wallace, J.; Lowe, M. Ground-Water Quality Classification Using GIS Contouring Methods for Cedar Valley, Iron County, Utah. *Digit. Mapp. Tech.* **2002**, *2*, 207.
48. Asadi, S.S.; Vuppala, P.; Reddy, M.A. Remote sensing and GIS techniques for evaluation of groundwater quality in municipal corporation of Hyderabad (Zone-V), India. *Int. J. Environ. Res. Public Health* **2007**, *4*, 45–52. [CrossRef]
49. Yammani, S. Groundwater quality suitable zones identification: Application of GIS, Chittoor area, Andhra Pradesh, India. *Environ. Earth Sci.* **2007**, *53*, 201–210. [CrossRef]